

# Photoinduced Electron Transfer of *N*-[(3- and 4-Diarylamino)phenyl]-1,8-Naphthalimide Dyads: Orbital-Orthogonal Approach in a Short-linked D–A System

Seiichiro Takahashi,<sup>†</sup> Koichi Nozaki,<sup>\*,‡</sup> Masatoshi Kozaki,<sup>†</sup> Shuichi Suzuki,<sup>†</sup> Kazutoshi Keyaki,<sup>‡</sup> Akio Ichimura,<sup>†</sup> Toshio Matsushita,<sup>†</sup> and Keiji Okada<sup>\*,†</sup>

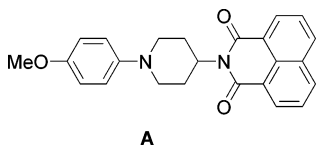
Department of Chemistry, Graduate School of Science, Osaka City University, Sugimoto, Sumiyoshi-ku, Osaka 558-8585, Japan, and Department of Chemistry, Graduate School of Science and Engineering, University of Toyama, 3190 Gofuku, Toyama 930-8555, Japan

Received: October 17, 2007; In Final Form: December 24, 2007

The photoinduced electron transfer of a series of meta- and para-linked triphenylamine–naphthalimide dyads, *N*-{3- and 4-[bis(4-*R*-substituted phenyl)amino]phenyl}-1,8-naphthalimide, **1m,p** (*R* = H), **2m,p** (*R* = Me), **3m,p** (*R* = OMe), and **4m,p** (*R* = NMe<sub>2</sub>) was investigated in toluene and DMF. The singlet charge-transfer (CT) states were observed in all cases. The decay rates were found to be faster in DMF ( $\tau = 6.5$  ps to 100 ps) than those in toluene ( $\tau = 190$  ps to 7 ns). The long-lived triplet CT states were observed in toluene for **3** (ca. 10% contribution,  $\tau = 670$  ns for **3m**, 240 ns for **3p**). No long-lived species were detected in DMF. The decay rates were somewhat faster in the para-isomers than in the meta-isomers in most cases. The photolysis of **5** (*p*-phenylene extended analogue of **3**, *R* = OMe) gave a singlet CT state and a locally excited triplet state on the naphthalimide chromophore.

## Introduction

Searching for systems of long-lived charge-separated states is an important subject in pure and applied sciences. An important goal is to create efficient artificial systems that function like natural photosynthetic systems where photoexcitation energy is efficiently converted to redox-chemical energy in the thylakoid membrane.<sup>1</sup> Recently, considerable developments have been made with multi-chromophoric systems including multistep electron transfer.<sup>2</sup> However, they did not always give long-lived charge-separated states. The most successful approach seems to be a spin control strategy using a chromophore undergoing rapid intersystem crossing.<sup>3</sup> This strategy leads to the selective formation of a triplet charge-separated state, which has a long lifetime (approximately microseconds) because of the spin-forbidden transition to the ground state. This method is also applicable to D–A dyads with a relatively short linkage<sup>3–5</sup> as demonstrated in a few systems including **A**.<sup>4b</sup>



The dyad **A**, reported by Verhoeven and co-workers, consists of the methoxyaniline (D) and naphthalimide (A) moieties, which are connected by a bridge of three sp<sup>3</sup>-carbon atoms. Irradiation of **A** (D–A) with a nanosecond laser pulse led to the formation of triplet charge-transfer (<sup>3</sup>CT) states characterized by a long lifetime ( $\tau \sim 1$   $\mu$ s) in relatively polar solvents. The

successful detection of <sup>3</sup>CT is due mainly to the fast intersystem crossing of the naphthalimide chromophore ( $D-^1A^* \rightarrow D-^3A^* \rightarrow ^3CT$ ).<sup>4b</sup>

Naphthalimide has a unique characteristic in its frontier molecular orbitals: there is a vertical nodal plane  $\sigma_v$  passing through the two central carbon atoms in the naphthalene ring and the nitrogen atom (Scheme 1). For this reason of symmetry, the electronic interaction between naphthalimide (radical anion) and the donor (radical cation) attached to the nitrogen atom of naphthalimide through spacers would be minimized. This would cause two advantageous effects in the primary processes of photoelectron transfer, in comparison to other acceptor-systems. (1) The rate of charge separation via a locally excited singlet state (<sup>1</sup>LE) on the naphthalimide chromophore would be suppressed, to give an increase in the quantum yield of the intersystem crossing of <sup>1</sup>LE (naphthalimide). (2) The rate of charge recombination would be retarded in both the singlet and the triplet states. Therefore, we expected that donors could be connected without a bridge to the nitrogen atom (naphthalimide). In this paper, we examined photoinduced electron transfer of *N*-[(3- and 4-diarylamino)phenyl]-1,8-naphthalimide dyads (**1–4**), where the substituted triphenylamine donor was directly combined to the naphthalimide chromophore, providing a novel *orbital-orthogonal* system in a short linked D–A system. Long-lived <sup>3</sup>CT were observed for **3** (*R* = OMe) and **4** (*R* = NMe<sub>2</sub>) in toluene. The effects of substituents, solvents, and topologies on the charge recombination were investigated and discussed.

## Experimental Section

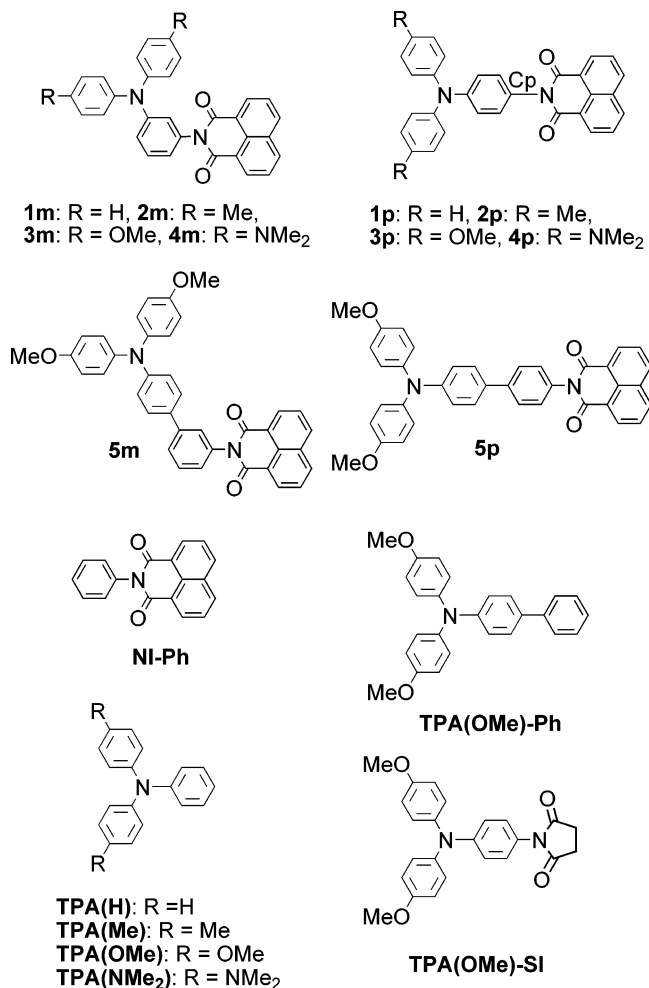
**Materials.** Syntheses of **3m** and **3p** are described as examples. Synthetic procedures and data for other compounds are given in Supporting Information (SI).

**Synthesis of *N*-{3-[Bis(4-anisyl)amino]phenyl}-1,8-naphthalimide (**3m**).** In a 100 mL two-necked flask, sodium *tert*-butoxide (247 mg, 2.57 mmol), Pd<sub>2</sub>(dba)<sub>3</sub>·CHCl<sub>3</sub> (177 mg, 0.171

\* Corresponding authors. K.N.: e-mail, nozaki@sci.u-toyama.ac.jp. K.O.: e-mail, okadak@sci.osaka-cu.ac.jp; tel, +81-6-6605-2568; fax, +81-6-6690-2709.

<sup>†</sup> Osaka City University.

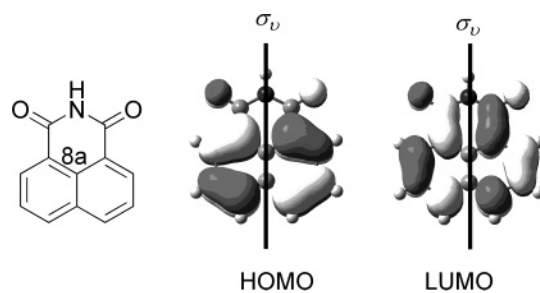
<sup>‡</sup> University of Toyama.



mmol), anhydrous toluene (50 mL), and a solution of P(<sup>t</sup>Bu)<sub>3</sub> in toluene (0.152 M, 0.40 mL, 0.0608 mmol) were stirred under nitrogen. To this mixture were added *N*-(3-bromophenyl)-1,8-naphthalimide (**6m**) (600 mg, 1.70 mmol) and dianisylamine (508 mg, 2.58 mmol). The mixture was refluxed overnight, allowed to cool and filtered through celite. The filtrate was concentrated under reduced pressure and passed through an alumina column and eluted with CH<sub>2</sub>Cl<sub>2</sub> to give almost pure **3m**. Recrystallization from ethanol gave analytically pure sample (305 mg, 38%). **3m:** a yellow powder; mp 262 °C; <sup>1</sup>H NMR (400 MHz, CDCl<sub>3</sub>) δ 8.62 (d, *J* = 7.8 Hz, 2H), 8.24 (d, *J* = 7.8 Hz, 2H), 7.77 (t, *J* = 7.8 Hz, 2H), 7.31 (t, *J* = 7.8 Hz, 1H), 7.14 (d, *J* = 9.0 Hz, 4H), 6.99 (d, *J* = 7.8 Hz, 1H), 6.85–6.81 (m, 5H), 6.77 (d, *J* = 7.8 Hz, 1H), 3.77 (s, 6H), IR (KBr) 1711, 1670, 1589, 1506, 1487, 1442, 1375, 1354, 1238, 1188, 1029, 833, 777 cm<sup>-1</sup>; MS(FAB<sup>+</sup>) *m/z* 500 [M<sup>+</sup>]. Anal. Calcd for C<sub>32</sub>H<sub>24</sub>N<sub>2</sub>O<sub>4</sub>: C 79.15, H 4.89, N 4.86. Found: C 78.96, H 4.77, N 4.79.

**Synthesis of *N*-{4-[Bis(4-anisyl)amino]phenyl}-1,8-naphthalimide (**3p**).** In a 100 mL two-necked flask, sodium *tert*-butoxide (259 mg, 2.70 mmol), Pd<sub>2</sub>(dba)<sub>3</sub>·CHCl<sub>3</sub> (184 mg, 0.178 mmol), anhydrous toluene (60 mL), and a solution of P(<sup>t</sup>Bu)<sub>3</sub> in toluene (0.152 M, 0.40 mL, 0.0608 mmol) were taken and stirred under a nitrogen atmosphere. To this mixture were added *N*-(4-bromophenyl)-1,8-naphthalimide (**6p**) (603 mg, 1.71 mmol) and dianisylamine (510 mg, 2.59 mmol). The mixture was refluxed overnight, allowed to cool and filtered through celite. The filtrate was concentrated under reduced pressure and passed through an alumina column eluted with CH<sub>2</sub>Cl<sub>2</sub> to give almost pure **3p**. Recrystallization from toluene gave

SCHEME 1



analytically pure sample (350 mg, 44%). **3p:** a yellow powder; mp 290 °C; <sup>1</sup>H NMR (400 MHz, CDCl<sub>3</sub>) δ 8.65 (d, *J* = 8.0 Hz, 2H), 8.26 (d, *J* = 8.0 Hz, 2H), 7.79 (t, *J* = 8.0 Hz, 2H), 7.16 (d, *J* = 9.2 Hz, 4H), 7.07 (d, *J* = 9.2 Hz, 2H), 7.02 (d, *J* = 9.2 Hz, 2H), 6.85 (d, *J* = 9.2 Hz, 4H), 3.81 (s, 6H); IR (KBr) 1705, 1665, 1587, 1504, 1462, 1437, 1373, 1358, 1313, 1288, 1238, 1188, 1038, 827, 781 cm<sup>-1</sup>; HRMS (*m/z*) calcd for C<sub>32</sub>H<sub>24</sub>N<sub>2</sub>O<sub>4</sub> 500.1736, found 500.1731.

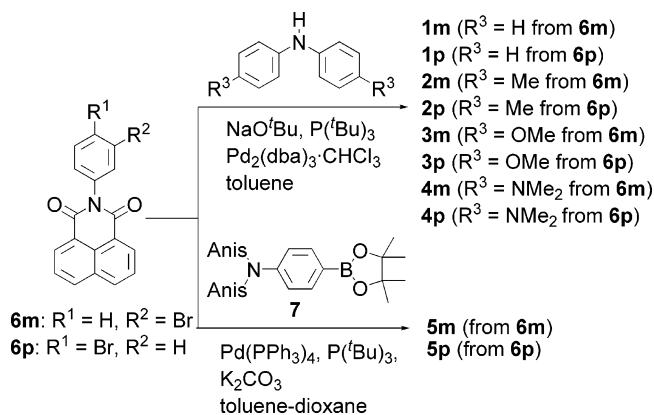
**Electrochemical Oxidation of Dyes 1–5.** For the assignment of transient species in the laser photolysis, the electrochemical oxidation of the reference compounds, **TPA(Me)**, **TPA(OMe)**, and **TPA(NMe<sub>2</sub>)** was carried out using an electrochemical cell (1 mm width with a fine mesh Pt working electrode) at suitable potentials generating the radical cation species in CH<sub>2</sub>Cl<sub>2</sub> in the presence of tetra-*n*-butylammonium hexafluorophosphate (0.1 M). The electrochemical reduction of *N*-phenyl-1,8-naphthalimide (**NI-Ph**) was also carried out in DMF under similar conditions. These data are shown in the SI.

**Laser Flash Photolyses of 1–5.** Nanosecond time-resolved difference spectra were obtained by using the third harmonic of a Q-switched Nd<sup>3+</sup>:YAG laser (Continuum Surelite I-10, λ = 355 nm).<sup>6</sup> Sample solutions in a 1 cm quartz cell were deaerated by bubbling with argon for 5 min. White light from a Xe-arc lamp was used for acquisition of absorption spectra. For measurements of picosecond time-resolved difference spectra, a sample solution in a quartz cell (2 mm length) was excited with the third harmonic pulses of a mode-locked Nd<sup>3+</sup>:YAG laser (Continuum PY61C-10).<sup>7</sup> The transient absorption spectra in the time range from –20 ps to 6 ns were acquired by using continuum pulses generated by focusing the fundamental laser pulse into a flowing H<sub>2</sub>O/D<sub>2</sub>O mixture (1:1 by volume). For the determination of emission lifetimes, samples were irradiated using the third harmonic pulses of the Nd<sup>3+</sup>:YAG laser. The emission from the samples was passed through a grating monochromator (H-10, Jobin Yvon) to eliminate scattering light and focused into a Si avalanche photodiode (Si-APD, S5139, Hamamatsu). The photocurrent from the Si-APD was amplified through wide-band amplifier (DC-500 MHz, CLC110) and accumulated on a digitizing oscilloscope (HP 54520 Hewlett-Packard) to get the decay-profile of the emission intensity, which was fit to single-exponential function with convolution of the instrumental response function of the measuring system. The time-resolution of the system is 2 ns.

## Results and Discussion

We use a general term of “CT” [charge-transfer = (D<sup>δ+</sup>–A<sup>δ-</sup>), δ ≤ 1] rather than “(D<sup>+</sup>–A<sup>-</sup>)”. As described later, transient species generated in DMF have similar absorptions to the free radical ions generated by the electrochemical method (radical cations in CH<sub>2</sub>Cl<sub>2</sub>, radical anions in DMF) and are well approximated as radical ion pairs [(D<sup>δ+</sup>–A<sup>δ-</sup>), δ = 1]. However, the transient species in toluene have similar but

## SCHEME 2



broader absorptions than those in DMF or the free radical ions, especially for the radical cation moieties. In addition, some of the short-lived transient species showed broad emission spectra, which is characteristic of singlet CT excited states. Thus, the species in toluene may be approximated as a CT complex with  $\delta$  close but not equal to unity.

**Syntheses of 1–5.** A series of triarylamine-naphthalimide dyads **1–5** with the meta- and para-topologies were synthesized through Pd(0)-mediated C–N bond formation<sup>8</sup> for **1–4** and by C–C bond formation<sup>9</sup> for **5** (Scheme 2). Synthetic details are described in the SI.

**Spectral Properties of 1–5.** The absorption spectra in the UV region are roughly similar to the spectral summation of the components, naphthalimide and triarylamine. For example, Figure 1 shows the electronic spectra of **3m** and **3p** with their components [NI-Ph and TPA(OMe)] (for other compounds see Figures S1–S5). The observed spectrum of **3m** is well approximated by a summation of the components [NI-Ph + TPA(OMe)], suggesting negligible electronic interaction in the ground state between the two components. This is ascribed to the meta-topology and the node of the frontier orbitals in naphthalimide. The observed spectrum of **3p** deviates in intensity around 340 nm from the spectral summation (Figure 1B), indicating that the donor part is conjugated with the nitrogen orbital but not with the naphthalimide chromophore because of the node of naphthalimide. Changing the model component from TPA(OMe) to TPA(OMe)-SI considerably improved the spectral similarity (Figure 1C). No charge-transfer band from the donor to the naphthalimide acceptor was observed.

These spectral features allow the estimation of the excitation (at 355 nm) ratios of naphthalimide chromophore for the meta-isomers, which vary considerably depending on the substrate, 78% for **1m**, 72% for **2m**, 65% for **3m**, 47% for **4m**, and 22% for **5m**. The corresponding values for the para-isomers are somewhat smaller than the meta-isomers<sup>10</sup> because of the perturbed red-shifted absorptions mainly on the nitrogen-substituted triphenylamine chromophores.

Judging from the longest edge of the absorption spectrum, the lowest locally excited singlet state (<sup>1</sup>LE) is likely to be on the naphthalimide chromophore for **1** and **2**, but on the triarylamine chromophore for **3** and **4**. Initially formed <sup>1</sup>LE states may undergo intramolecular energy transfer and/or electron-transfer reactions. These processes should occur very rapidly. In fact, the species observed in the pico-second laser photolysis was exclusively <sup>1</sup>CT states and no <sup>1</sup>LE state on the naphthalimide or triarylamine chromophores was observed. Singlet energies [ $E_s(^1\text{LE})$ ] of these dyads are estimated from the absorption edges and summarized in Table 2.

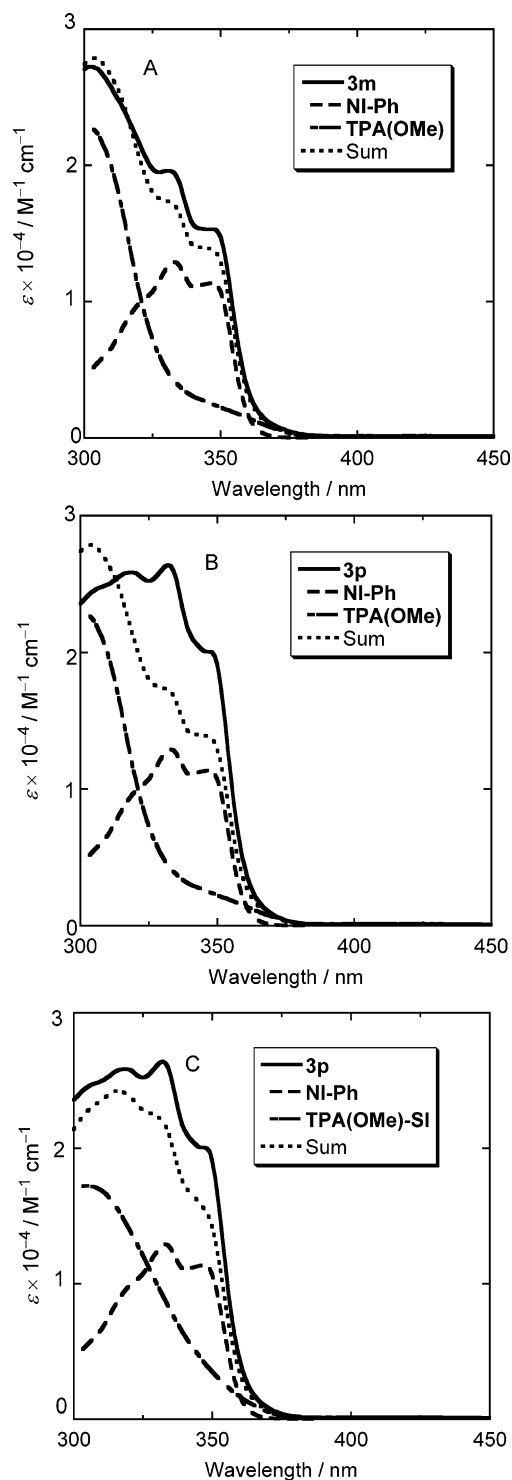


**Figure 1.** UV-vis absorption spectra of **3m** and **3p** and their components: (A) **3m** + TPA(OMe); (B) **3p** + TPA(OMe); (C) **3p** + TPA(OMe)-SI in toluene.

NI-Ph is known to exhibit weak fluorescence.<sup>11</sup> Recently, Bérces, Kossanyi, and co-workers have reported that some donor-substituted naphthalimides show fluorescence with a large Stokes-shift.<sup>12</sup> The emitting state was found to have a large CT character. The singlet CT state is the most plausible state emitting the fluorescence. Similar fluorescence was observed for **1**, **2**, **3**, and **5** in toluene (Figures S6–S9): The weak emissions were observed for instance at  $\lambda_{\text{EMmax}} = 700$  nm for **3m**, which is different from fluorescence of NI-Ph (350–500 nm with  $\lambda_{\text{EMmax}} \sim 400$  nm, Figure S10) or of the donor part (TPA(OMe)) (360–450 nm with  $\lambda_{\text{EMmax}} = 386$  nm, Figure

**TABLE 1: Redox Potentials (V vs Fc/Fc<sup>+</sup>) of 1–5 in CH<sub>2</sub>Cl<sub>2</sub> and DMF**

compd	CH <sub>2</sub> Cl <sub>2</sub>		DMF	
	$E_{ox}/V^a$	$E_{red}/V^a$	$E_{ox}/V^a$	$E_{red}/V^a$
<b>1m</b>	+0.60	-1.82	+0.57	-1.72
<b>1p</b>	+0.59	-1.82	+0.57	-1.72
<b>2m</b>	+0.45	-1.82	+0.49	-1.71
<b>2p</b>	+0.45	-1.81	+0.48	-1.73
<b>3m</b>	+0.27	-1.84	+0.33	-1.72
<b>3p</b>	+0.26	-1.85	+0.32	-1.73
<b>4m</b>	-0.20	-1.84	-0.13	-1.72
<b>4p</b>	-0.20	-1.84	-0.14	-1.73
<b>5m</b>	+0.21	-1.82	+0.28	-1.71
<b>5p</b>	+0.20	-1.82	+0.29	-1.71

<sup>a</sup> vs Fc/Fc<sup>+</sup> using a glassy carbon as a working electrode with sweep rate of 100 mV/s in the presence of tetra-*n*-butylammonium hexafluorophosphate.

**TABLE 2: Energy Levels of the Lowest Excited Singlet ( $E_S$ ) and Triplet ( $E_T$ ) States and the Radical Ion Pair State ( $\Delta G_{rip}$ ) above the Ground State ( $E_{GS} = 0$ )**

compd	$E_S$ ( <sup>1</sup> LE)/eV <sup>a</sup>	$E_T$ ( <sup>3</sup> LE)/eV <sup>b</sup>	$\Delta G_{rip}/eV^c$ in toluene	$\Delta G_{rip}/eV^d$ in DMF
<b>1m</b>	3.43	2.27	2.50	2.24
<b>1p</b>	3.43	2.27	2.59	2.24
<b>2m</b>	3.43	2.27	2.35	2.15
<b>2p</b>	3.43	2.27	2.44	2.16
<b>3m</b>	3.40	2.27	2.19	2.00
<b>3p</b>	3.39	2.27	2.28	2.00
<b>4m</b>	3.23	— <sup>e</sup>	1.72	1.54
<b>4p</b>	3.22	— <sup>e</sup>	1.82	1.54
<b>5m</b>	3.26	2.27	2.40	1.96
<b>5p</b>	3.25	2.27	2.44	1.97

<sup>a</sup> Estimated by the absorption edge at the 1/10th height of the maximal height of the longest absorption in toluene. <sup>b</sup> Determined from the 0–0 band of the phosphorescence in glassy toluene at 77 K. <sup>c</sup> Using eq 1 ( $\epsilon = 2.38$  for toluene,  $\epsilon_{ref} = 8.93$  for CH<sub>2</sub>Cl<sub>2</sub>). <sup>d</sup> Calculated using the redox potentials in DMF. <sup>e</sup> The phosphorescence was not observed.

S13). The observed emissions are assigned as those from <sup>1</sup>CT states, which suggest the rapid transition from <sup>1</sup>LE (naphthalimide chromophore) to <sup>1</sup>CT in the excited-state surface. No such CT fluorescence was observed for **4** in toluene and for all dyads in DMF. The lifetimes of the CT-emissions are summarized in Table 4.

Naphthalimide exhibits phosphorescence in glassy toluene at 77 K with vibronic spacing of 1470 cm<sup>-1</sup> and with the 0–0 band at 547 nm from which the triplet energy ( $E_T$ ) of <sup>3</sup>LE on naphthalimide was determined to be 2.27 eV (Figure S16).<sup>13</sup> The donor moieties had higher triplet energies as determined from the 0–0 band of the phosphorescence of the reference compounds;  $E_T = 3.00$  eV for **TPA(H)**, 2.97 eV for **TPA(Me)**, 2.88 eV for **TPA(OMe)**, and 2.52 eV for **TPA(OMe)-Ph** (Figure S17). Dyads **1**, **2**, **3**, and **5** exhibited an identical phosphorescence spectrum with that from the naphthalimide chromophore in glassy toluene (Figures S18–S21). These observations are consistent with the free energy analyses showing that the lowest triplet state should be <sup>3</sup>LE on the naphthalimide chromophore for **1**, **2**, and **5** in toluene ( $\Delta G_{rip}$  in Table 2 and  $E_{CT}$  in Table 3, *vide infra*). The analyses show, however, that the energy of the radical ion-pair state ( $\Delta G_{rip}$  and  $E_{CT}$ ) for **3** is located in a similar energy level to <sup>3</sup>LE. The transient spectra in the laser photolysis clearly indicate that <sup>3</sup>CT is the lowest triplet state at room temperature in solution for **3** (*vide infra*). Therefore, the finding of the phosphorescence from <sup>3</sup>LE (naphthalimide) for **3** suggests that <sup>3</sup>CT has a higher

**TABLE 3: Energy of <sup>1</sup>CT State ( $E_{CT}$ ), Fluorescence Maximum ( $E_{EM}$ ), and the Reorganization Energy ( $\lambda_{CT}$  and  $\lambda_s$ ) for <sup>1</sup>(D<sup>•+</sup>–A<sup>•-</sup>) → GS<sup>a</sup>**

compd	toluene				DMF $\lambda_s^e$
	$E_{CT}^b$	$E_{EM}^c$	$\lambda_{CT}^d$	$\lambda_s^e$	
<b>1m</b>	2.48	1.83	0.65	0.03	0.44
<b>1p</b>	2.43	1.79	0.64	0.03	0.55
<b>2m</b>	2.38	1.73	0.65	0.03	0.44
<b>2p</b>	2.38	1.72	0.66	0.03	0.55
<b>3m</b>	2.21	1.55	0.66	0.03	0.44
<b>3p</b>	2.25	1.59	0.66	0.03	0.55
<b>4m</b>	— <sup>f</sup>	— <sup>f</sup>	— <sup>f</sup>	0.03	0.44
<b>4p</b>	— <sup>f</sup>	— <sup>f</sup>	— <sup>f</sup>	0.03	0.55
<b>5m</b>	2.43	1.77	0.66	0.05	0.76
<b>5p</b>	2.44	1.78	0.66	0.05	0.82

<sup>a</sup> Energies given in eV unit. <sup>b</sup> Determined from the onset of the CT-fluorescence with an error of  $\pm 0.05$  eV. <sup>c</sup> Determined from the emission maximum energy in the plot of  $f_{CT}(\tilde{\nu})/\tilde{\nu}^3$  vs  $\tilde{\nu}$ , where  $f_{CT}(\tilde{\nu})$  denotes CT fluorescence spectrum as a function of wavenumber  $\tilde{\nu}$ . <sup>d</sup> Calculated using eq 2 with an error of  $\pm 0.05$  eV. <sup>e</sup> Calculated using eq 3 with  $\epsilon = 2.38$  and  $n^2 = 2.24$  for toluene, and  $\epsilon = 36.7$  and  $n^2 = 2.05$  for DMF. <sup>f</sup> Not observed.

**TABLE 4: Lifetimes of Transient Species Assigned to CT or LE by Transient Absorption ( $\tau$ ) and Transient Emission ( $\tau_f$ ) Measurements for the Photolysis of 1–5**

compd	lifetimes of short-lived component ( $\tau$ ) and CT-fluorescence ( $\tau_f$ )			lifetime of long-lived component [ <sup>3</sup> LE or <sup>3</sup> CT]	
	toluene			toluene	DMF
	$\tau$	$\tau_f$	DMF		
<b>1m</b>	7 ns	5 ns	n.m.	<sup>3</sup> LE, n.d.	n.m.
<b>1p</b>	2 ns	$\leq 2$ ns	n.m.	<sup>3</sup> LE, n.d.	n.m.
<b>2m</b>	7 ns	7 ns	100 ps	<sup>3</sup> LE, 12.0 $\mu$ s	n.o.
<b>2p</b>	2 ns	$\leq 2$ ns	46 ps	<sup>3</sup> LE, 3.3 $\mu$ s	n.o.
<b>3m</b>	4 ns <sup>a</sup>	3 ns	20 ps	<sup>3</sup> CT, 670 ns <sup>a</sup>	n.o.
<b>3p</b>	2 ns <sup>b</sup>	$\leq 2$ ns	11 ps	<sup>3</sup> CT, 240 ns <sup>b</sup>	n.o.
<b>4m</b>	190 ps	n.m.	6.8 ps	<sup>3</sup> CT, — <sup>c</sup>	n.o.
<b>4p</b>	220 ps	n.m.	6.5 ps	<sup>3</sup> CT, — <sup>c</sup>	n.o.
<b>5m</b>	9 ns	7 ns	19 ps	<sup>3</sup> LE, n.d.	n.o.
<b>5p</b>	5 ns	5 ns	16 ps	<sup>3</sup> LE, n.d.	n.o.

<sup>a</sup> With a fraction ratio of 92 (short-lived component):8 (long-lived component). <sup>b</sup> With a fraction ratio of 87 (short-lived component):13 (long-lived component). <sup>c</sup> Less than 1% fraction. n.m.: not measured. n.d.: not determined. n.o.: not observed

energy than <sup>3</sup>LE (naphthalimide) in glassy toluene at 77 K, where the solvated stabilization of CT is lesser available.<sup>14</sup> It should be noted that  $\Delta G_{rip}$  in DMF is lower than the energy level of <sup>3</sup>LE (naphthalimide, 2.27 eV) for all compounds. This is consistent with the observations that <sup>1</sup>CT decayed rapidly to the ground state and no <sup>3</sup>LE (naphthalimide) was detected in DMF (*vide infra*). Compound **4** (R = NMe<sub>2</sub>) exhibited no phosphorescence at 77 K in toluene, suggesting that the lowest triplet state of **4** is not <sup>3</sup>LE but a nonemissive <sup>3</sup>CT state.

**Molecular Orbital Calculations for 1–5.** To determine the most stable conformation, the conformers with different torsion angles between the phenyl rings and with different orientations of methoxy groups were systematically generated and minimized (AM1) using Spartan.<sup>15</sup> For the most stable conformer, TD-DFT/6-31G(d) calculations were carried out to determine the transition character for the singlet excited states (SI).<sup>16</sup> Figure 2 shows the HOMO and LUMO for **3m** and **3p** for example, showing that the HOMO is localized on the donor (triarylamine) part and the LUMO on the acceptor part (naphthalimide). The first excited singlet state was shown to be mainly the HOMO  $\rightarrow$  LUMO transition, indicating that the first excited singlet state is the CT state.

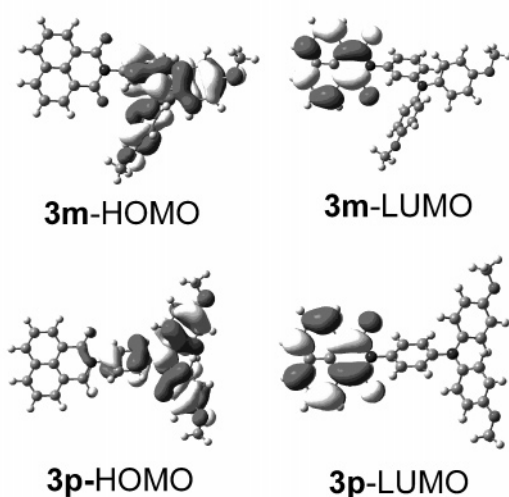


Figure 2. HOMO and LUMO of **3m** and **3p**.

### Redox Potentials and Estimation of Free Energies for 1–5.

The redox potentials of these dyads were measured by means of cyclic voltammetry in both  $\text{CH}_2\text{Cl}_2$  and DMF with a SCE reference electrode. Then, all the redox potentials were corrected by the ferrocene-ferrocenium potential ( $\text{Fc}/\text{Fc}^+$ : +0.430 V vs SCE in  $\text{CH}_2\text{Cl}_2$ , +0.47 V in DMF). These values are summarized in Table 1.

The free energy change for the formation of radical ion pair states ( $\Delta G_{\text{rip}}$  in eV) from the ground states in toluene was roughly estimated using the Weller approximation (eq 1);<sup>17</sup> the radical ion pair state is considered as a solvent-separated one with a center(+)-to-center(−) distance  $R$  (in angstrom) and the effective radii  $r$  (in angstrom) equals for donor (D) and acceptor (A).  $\epsilon$  is a dielectric constant of the solvent and  $\epsilon_{\text{ref}}$  (in this case  $\epsilon_{\text{ref}} = 8.93$  for  $\text{CH}_2\text{Cl}_2$ ) is that in the reference solvent in which  $E_{\text{ox,ref}}$  (D) and  $E_{\text{red,ref}}$  (A) are measured. The free energy change for the back electron transfer to the ground state ( $\Delta G_{\text{bet}}$ ) is expressed as that of the opposite sign.  $R$  was approximated

$$\Delta G_{\text{rip}} = -\Delta G_{\text{bet}} = E_{\text{ox,ref}}(\text{D}) - E_{\text{red,ref}}(\text{A}) - 14.4/(\epsilon R) + (14.4/r)(1/\epsilon - 1/\epsilon_{\text{ref}}) \quad (1)$$

as a distance between the carbon atom at the 8a position (Scheme 1) and the central nitrogen atom of the triarylamine structure; 7.5 Å for **1m**, **2m**, **3m**, **4m**, 8.5 Å for **1p**, **2p**, **3p**, **4p**, 11.7 Å for **5m**, and 12.9 Å for **5p**. The effective ionic radii  $r$  of the donor and the acceptor moieties were assumed to be 5 Å.<sup>17b</sup> Table 2 summarizes the  $\Delta G_{\text{rip}}$  values in toluene and DMF with the  $E_{\text{S}}$  and  $E_{\text{T}}$  values.

Table 2 indicates that the lowest triplet state is <sup>3</sup>LE state for **1**, **2**, and **5**, but <sup>3</sup>CT state for **4** in toluene. For **3**, <sup>3</sup>LE and <sup>3</sup>CT states are in similar energies in the same solvent. In spite of rough approximation for the estimation methodology (eq 1), these results are in good accord with the experimental estimation of the energy levels of charge transfer state ( $E_{\text{CT}}$ , Table 3) estimated from the onset of the CT fluorescence (*vide supra*, Figures S6–S9). The absence of phosphorescence (77 K in toluene) for **4** suggests the lowest <sup>3</sup>CT state (*vide supra*).

Using the  $E_{\text{CT}}$  or  $\Delta G_{\text{rip}}$  values, reorganization energy ( $\lambda_{\text{CT}}$ ) for the back charge-transfer process (CT  $\rightarrow$  GS) can be calculated by<sup>18</sup>

$$\lambda_{\text{CT}} = E_{\text{CT}} - E_{\text{EM}} \quad (2)$$

$E_{\text{EM}}$  is the emission maximum energy in the plot of  $f_{\text{CT}}(\tilde{\nu})/\tilde{\nu}^3$  vs  $\tilde{\nu}$ , where  $f_{\text{CT}}(\tilde{\nu})$  denotes CT fluorescence spectrum as a function of wavenumber  $\tilde{\nu}$  (Table 3). As shown in Table 3, the  $\lambda_{\text{CT}}$  values in toluene are about 0.66 eV. The  $\lambda_{\text{CT}}$  value can be formally divided into internal ( $\lambda_{\text{i}}$ ) and solvent ( $\lambda_{\text{s}}$ ) reorganization energies:  $\lambda_{\text{CT}} = \lambda_{\text{i}} + \lambda_{\text{s}}$ . Two-spheres in a dielectric continuum model allows a crude estimation of the  $\lambda_{\text{s}}$  value (eV), that is,<sup>19</sup>

$$\lambda_{\text{s}} = 14.4(\Delta e)^2 \left( \frac{1}{n^2} - \frac{1}{\epsilon} \right) \left( \frac{1}{2r_{\text{A}}} + \frac{1}{2r_{\text{D}}} - \frac{1}{R} \right) \quad (3)$$

where  $\Delta e$  is number of transferred electrons,  $n$  is refractive index,  $r_{\text{A}}$  and  $r_{\text{D}}$  denote radius of the acceptor and the donor, respectively. Table 3 summarizes the  $\lambda_{\text{s}}$  values calculated for toluene and for DMF assuming  $r_{\text{A}}$  and  $r_{\text{D}}$  equal to 5.0 Å for all the dyads. Very small  $\lambda_{\text{s}}$  values for toluene indicate that internal ( $\lambda_{\text{i}}$ ) contribution is dominant in  $\lambda_{\text{CT}}$ . The solvent reorganization energies were estimated to be considerably large in DMF: 0.5 eV for **1–4**, 0.8 eV for **5**.

**Outline of Laser Photolysis.** In accordance with the energy consideration,  $E_{\text{S}} > \Delta G_{\text{rip}}$  (Table 2) or  $E_{\text{CT}}$  (Table 3), the excitation of **1–4** gave <sup>1</sup>CT in both nonpolar (toluene) and polar (DMF) solvents. The lowest triplet states of **1** ( $R = \text{H}$ ) and **2** ( $R = \text{Me}$ ) are predicted to be not <sup>3</sup>CT but <sup>3</sup>LE (naphthalimide) in toluene, whereas they are <sup>3</sup>CT in DMF. The transient spectra obtained from the excitation (at 355 nm) of dyads **1** and **2** showed a similar time profile; the absorption of <sup>3</sup>LE was observed after the decay of <sup>1</sup>CT states. The detailed analysis was achieved for **2**. Dyads **3** ( $R = \text{OMe}$ ) have a small energy difference between <sup>3</sup>CT and <sup>3</sup>LE. The expected <sup>3</sup>CT with a long lifetime was observed after decay of <sup>1</sup>CT in toluene, whereas exclusive decay of <sup>1</sup>CT to the ground state was observed in DMF. Compounds **4** ( $R = \text{NMe}_2$ ) have lower  $\Delta G_{\text{rip}}$  values than compounds **3**. Although the long-lived <sup>3</sup>CT states were detected, the contribution of <sup>3</sup>CT was very small for **4**. For compounds **5** (phenylene-extended analogue of **3**), the lowest <sup>3</sup>LE state was observed after the decay of <sup>1</sup>CT in toluene, whereas no long-lived species was detected in DMF. The results for **5** are separately described as a distance effect. The observed lifetimes of <sup>1</sup>CT for **1–5** and <sup>3</sup>CT for **3** are summarized in Table 4. These results are separately described below.

**Laser Photolysis for 1m, 2m, 1p, and 2p in Toluene.** Excitation with a nanosecond laser pulse (355 nm, fwhm: 4 ns) allows selective excitation [78% for **1m**, 72% for **2m**] of the naphthalimide chromophore. The time dependencies of the transient absorption spectra of **1m** and **2m** were similar. Figure 3 shows the transient absorption spectra of **2m** in toluene (Figure S27 for **1m** and **1p**). After excitation, strong new absorptions appeared at  $\lambda_{\text{max}} = 420$  and 660 nm. The 420 nm absorption is a characteristic band of the anion radical of naphthalimide moiety (Figure S22 for the electrochemical reduction of **NI-Ph** in DMF).<sup>4b</sup> The 660 nm absorption band is similar to the absorption of the free ditolylphenylamine radical cation generated by the electrochemical method **TPA(Me)**<sup>+</sup> in  $\text{CH}_2\text{Cl}_2$  [ $\lambda_{\text{max}} = 684$  nm, 560 nm (sh), (Figure S23)] but broader than the free radical cation in  $\text{CH}_2\text{Cl}_2$ . Both bands (420 nm, 660 nm) decayed exponentially with a single lifetime of  $\tau = 7$  ns for both **1m** and **2m**. Furthermore, these lifetimes were very close to those observed for the CT emission ( $\tau_{\text{f}}$  in Table 4). Thus, the observed absorption spectra (Figure 3) are assigned to be the <sup>1</sup>CT states. The <sup>1</sup>CT absorptions had almost disappeared 100 ns after the laser excitation. The remaining species had an absorption band at 470 nm, which was assigned to the T–T absorption of <sup>3</sup>LE on the naphthalimide chromophore.<sup>4b</sup> The time dependencies of these transient species are shown in Figure

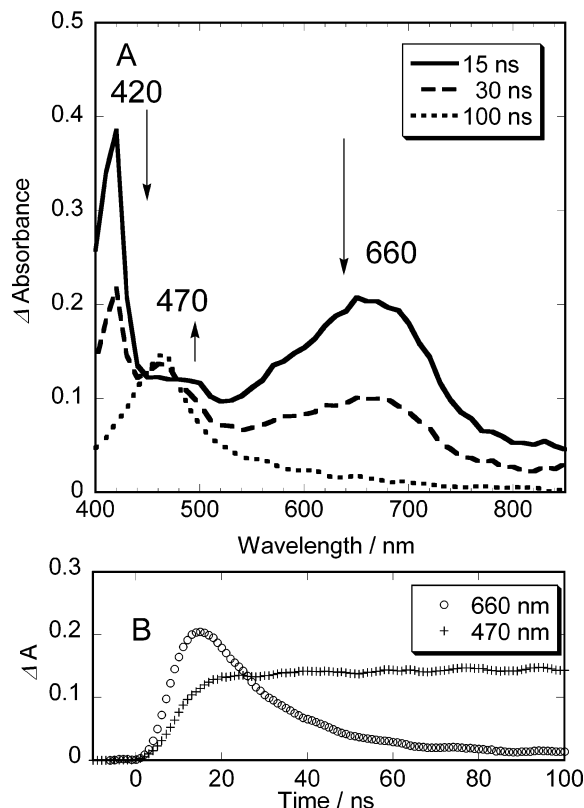


**Figure 3.** Transient spectra of **2m** after excitation of a nanosecond laser pulse (355 nm, fwhm: 4 ns) (A) and the decay curves monitored at 470 and 660 nm (B) in toluene.

3B. The absorbance at 470 nm was almost constant in the decay of  $^1\text{CT}$ . Two explanations are possible: This may be because of the small difference of molar absorptivities between  $^3\text{NI}$  ( $\epsilon_{470} \sim 10\,000$ )<sup>20</sup> and the summation of  $\text{NI}^-$  ( $\epsilon_{470} \sim 4700$ ) and  $\text{TPA}(\text{Me})^+$  ( $\epsilon_{470} \sim 3900$ ). The kinetic analysis of the time-profiles for **2m** with convolution of the instrumental function indicates that the initial concentration of  $^1\text{CT}$  ( $\epsilon_{420} \sim 27\,000$  for  $\text{NI}^-$ ) is nearly comparable to the final concentration of  $^3\text{LE}$  ( $\epsilon_{470} \sim 10\,000$ ). Thus, this consideration is compatible with the mechanism of intersystem crossing involving the back electron transfer,  $^1\text{CT} \rightarrow ^3\text{LE}$ .<sup>21</sup> However, the time dependencies in Figure 3B are also compatible with the mechanism involving a fast intersystem crossing within the naphthalimide chromophore,  $^1\text{LE} \rightarrow ^3\text{LE}$ .<sup>22</sup> The differentiation of these mechanisms is difficult at present.

The formation of  $^1\text{CT}$  and/or  $^3\text{LE}$  on the naphthalimide could not be observed even in picosecond laser photolysis (Figure S29A), indicating that both processes occur much faster than the limit of time resolution of our apparatus, 5 ps.

The time dependencies of the transient absorptions for the para-isomers, **1p** (Figure S27B) and **2p** (Figure 4 and S29B) in toluene were essentially similar to those for the meta-isomers, **1m** and **2m**, although the transient absorptions appeared at a considerably longer wavelength ( $\sim 850$  nm for **2p** in Figure 4 and S29). The broad 850 nm absorption may be partly due to the overlap of the radical cation and the naphthalimide radical anion, which appears around 840 nm in DMF (Figure S22). The decays of  $^1\text{CT}$  ( $\tau \sim 2$  ns for both **1p** and **2p**) were somewhat faster than those for the meta-isomers ( $\tau = 7$  ns for both **1m** and **2m**, Table 4).

**Laser Photolysis of 3m and 3p in Toluene.** The spectroscopic feature of **3** is not much different from **1** and **2**. However, because of the electron-donating property of the methoxy group,

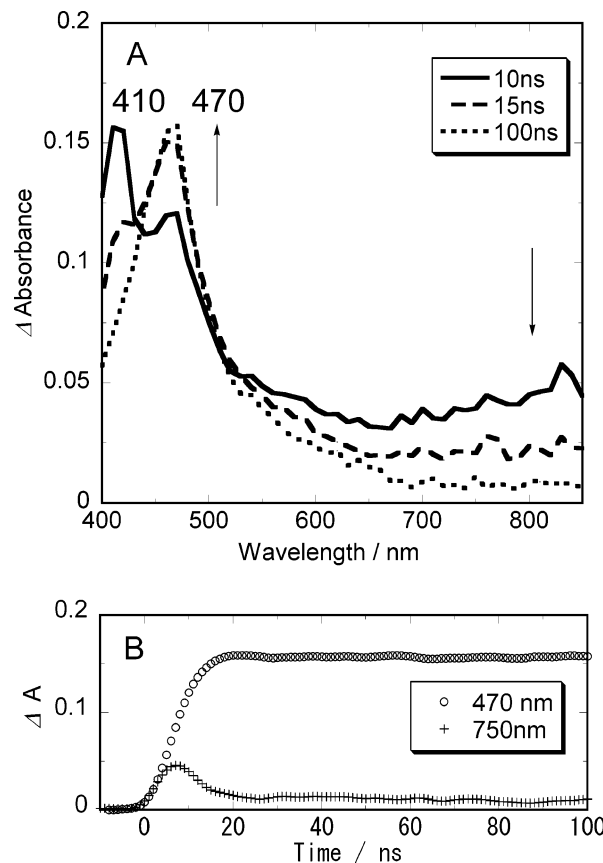


**Figure 4.** Transient spectra of **2p** after excitation of a nanosecond laser pulse (355 nm, fwhm: 4 ns) (A) and the decay curves monitored at 470 and 750 nm (B) in toluene.

the energy levels of CT states of **3m** and **3p** are lower than those of **1** and **2**:  $\Delta G_{\text{rip}}$  (2.19, 2.28 eV in Table 2) or  $E_{\text{CT}}$  (2.21, 2.25 eV in Table 3) for **3** in toluene are comparable to the level of  $^3\text{LE}$  ( $E_{\text{T}} \sim 2.27$  eV, Table 2). Figure 5A shows the transient absorption spectra for the excitation of **3m**. The observed absorptions are reasonable as  $^1\text{CT}$ ; naphthalimide radical anion ( $\lambda_{\text{max}} = 420, 490$  nm) and the donor radical ( $\lambda_{\text{max}} = 720$  nm with a broader width) in comparison with the electrochemically generated dianisylphenylamine radical cation  $[\text{TPA}(\text{OMe})^+]$ ,  $\lambda_{\text{max}} = 755$  nm in  $\text{CH}_2\text{Cl}_2$ , Figure S24). Importantly, the decay curves of the cationic and anionic species are consistently expressed as double exponential functions (Figure 5B), showing fast major (ca 92%) decay of  $\tau = 4$  ns and slow minor (ca 8%) decay of  $\tau = 670$  ns. After 50 ns the species is almost all of the long lifetime, which has an identical spectral pattern with the fast decaying species. The lifetime of the fast component is almost the same as that for the CT fluorescence ( $\tau_{\text{f}}$  in Table 4). These results strongly indicate that the species of the short lifetime and the long lifetime are ascribed to  $^1\text{CT}$  and  $^3\text{CT}$ , respectively. The fast decaying transient component,  $^1\text{CT}$ , was also observed in picosecond-laser excitation: the spectra observed later than between 200 ps and 6 ns (Figure S31) were consistent with those obtained in the nanosecond-pulse excitation. Similar results were obtained for the photolysis of **3m** in dioxane ( $\lambda_{\text{max}} = 410, 490, 720$  nm with  $\tau \sim 3$  ns with 96% contribution, 800 ns with 4% contribution in Figure S32).

Transient absorption spectra for the photolysis of the para-isomer (**3p**) in toluene showed an essentially similar time-dependence (Figure 6,  $\tau \sim 2$  ns with 87% contribution, 240 ns with 13% contribution). The absorption assigned to the donor radical cation ( $\lambda_{\text{max}} = 710$  nm) in toluene accompanied the longer absorption ( $\lambda_{\text{max}} = 840$  nm), which may be partly due

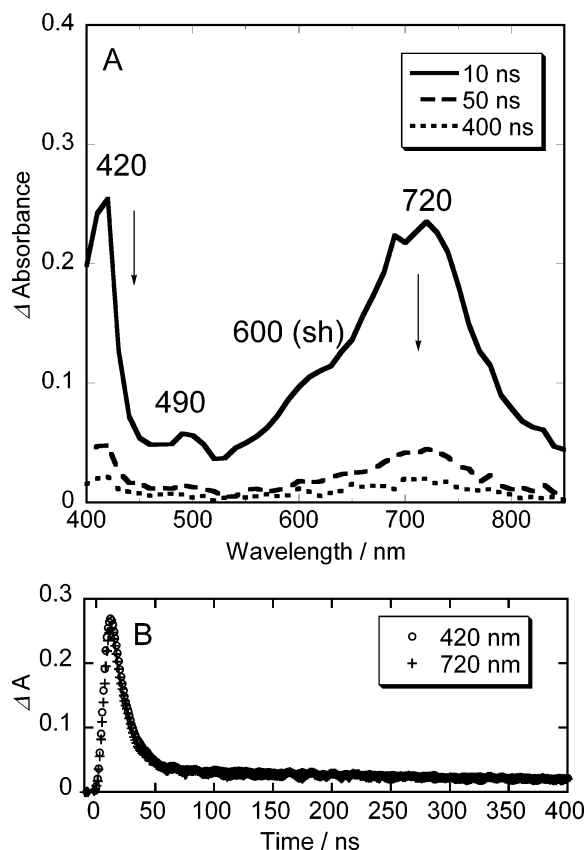


**Figure 5.** Transient spectra of **3m** after excitation of a nanosecond laser pulse (355 nm, fwhm: 4 ns) (A) and the decay curves monitored at 420 and 720 nm (B) in toluene.

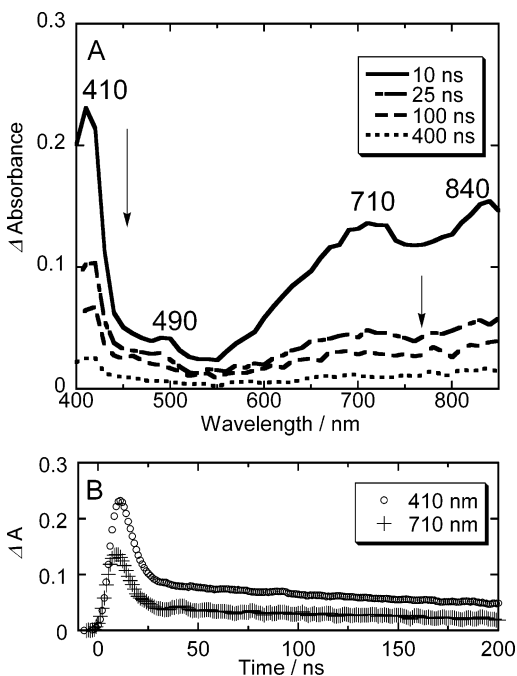


**Figure 6.** Transient spectra of **3p** after excitation of a nanosecond laser pulse (355 nm, fwhm: 4 ns) (A) and the decay curves monitored at 410 and 710 nm (B) in toluene.

to naphthalimide radical anion (420, 840 nm in DMF).<sup>4b</sup> However, the absorption at 840 nm was significantly larger than that expected from the naphthalimide radical anion absorption, for a reason not clear at present. In dioxane, normal absorptions were observed ( $\lambda_{\text{max}} = 410, 490, 720$  nm with  $\tau \sim 3$  ns with 96% contribution, 540 ns with 7% contribution in Figure S32).

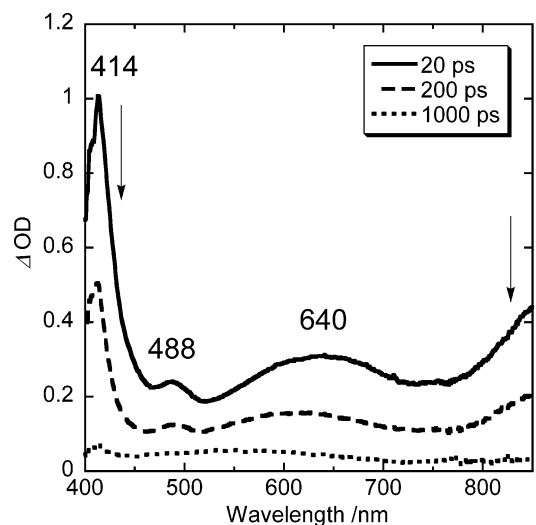


**Figure 7.** Transient spectra of **4m** after excitation of a picosecond laser pulse (355 nm, fwhm: 17 ps) in toluene.

Two mechanisms are possible in principle for the formation of long-lived  $^3\text{CT}$ : one involves a rapid intersystem crossing of  $^1\text{LE}$  (naphthalimide) via the spin-orbit coupling within the naphthalimide chromophore,  $[\text{TPA}(\text{OMe})\text{-}^1\text{NI}] \rightarrow [\text{TPA}(\text{OMe})\text{-}^3\text{NI}] \rightarrow ^3\text{CT}$ , the other involves an intersystem crossing within the CT states,  $[\text{TPA}(\text{OMe})\text{-}^1\text{NI}] \rightarrow ^1\text{CT} \rightarrow ^3\text{CT}$ . The latter process has been observed in weakly coupled D-A systems ( $|2J| < \text{hyperfine coupling}$ )<sup>2b,3b,23</sup> and would be unexpected in the present system where the S-T gap is increased by the proximity of the donor and acceptor, prohibiting significant S-T mixing. The former process has an electron-transfer step with  $\Delta G \sim 0.0$  eV in the second step. The reaction would proceed efficiently because of the long lifetime of  $^3\text{NI}$ .

**Laser Photolysis of 4m and 4p in Toluene.** The oxidation potentials of **4** are much lower than those of **1**, **2**, and **3**. As a result, the ion pair energies are considerably lower than  $^3\text{LE}$  (naphthalimide). In the case of **4**, fast decay from  $^1\text{CT}$  was predominantly observed. Figure 7 shows the transient absorption spectra after picosecond-laser excitation of **4m** in toluene. The 414 and 488 nm absorptions are assigned to an anion radical of the naphthalimide moiety. The electrochemical oxidation of **TPA**(NMe<sub>2</sub>) gave rise to a small band at 560 nm and an intense band at 1057 nm as the radical cation bands (Figure S25). The intense band at 1057 nm is over our detector range in the transient absorption experiments. The gradual increase of the intensity of the transient absorption from 800 to 900 nm is indicative of the stronger absorption over 1000 nm. The lifetime of  $^1\text{CT}$  was estimated to be 190 ps from the decay of absorption at 414 nm for **4m**. A slow and minor decaying component (<1%) attributable to  $^3\text{CT}$  was also observed in the nanosecond laser excitation in toluene [ $\tau = 920$  ns (420 nm) for **4m**, 780 ns (420 nm) for **4p**, Figure S34]. The small fraction of  $^3\text{CT}$  for **4** suggests that the photochemical charge separation from  $^1\text{NI}$  in **4** is faster than that in **3**. Then, the intersystem crossing within the **NI** chromophore of **4** becomes less competitive than that of dyad **3**, resulting in a lower  $^3\text{CT}$  intensity from  $^3\text{NI}$  for **4**.

**Summary of Laser Photolysis of 1-4 in Toluene.** The electron donating substituents in the donor moiety certainly decrease the CT energy ( $\Delta G_{\text{rip}}$  in Table 2 or  $E_{\text{CT}}$  in Table 3). The  $\Delta G_{\text{rip}}$  values of **1-4** are 2.6-1.7 eV above the ground state. These values are far beyond the reorganization energy ( $\lambda_{\text{CT}} \sim 0.7$  eV, Table 3). Therefore, the back electron-transfer processes in the present system must be deep in the Marcus inverted region. The  $\Delta G_{\text{rip}}$  value gradually decreases in the order of **1**

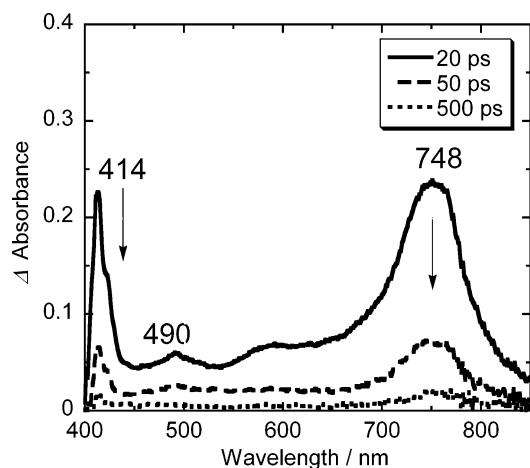


**Figure 8.** Transient spectra of **3m** after excitation of a picosecond laser pulse (355 nm, fwhm: 17 ps) in DMF.

(2.5–2.6 eV) → **2** (2.3–2.4 eV) → **3** (2.2–2.3 eV) and drops significantly in **4** (1.7–1.8 eV). The lifetimes are similar for **2–7** ns for **1–3**, but considerably shorter (190–220 ps) for **4**. The shorter lifetime for **4** qualitatively accords with the small effect in the Marcus inverted region.<sup>4</sup> According to Marcus theory, the electron-transfer rate constant maximizes when the electrostatic energy released in the reaction (free energy change,  $\Delta G_{\text{rip}}$ ) equals to the energy required for the geometrical changes of the system including surrounding (reorganization energy,  $\lambda_{\text{CT}}$ ). In the Marcus inverted region, internal vibrational modes must accept the excess energy through nuclear tunneling effects and thus Franck–Condon weighted density-of-states of the transition decreases as the excess energy increases. The excess energy ( $\Delta G_{\text{rip}} - \lambda_{\text{CT}}$ ) in the Marcus inverted region is calculated to be 1.6 eV for **3**, 1.7 eV for **2**, 1.8 eV for **1**, and  $\sim 1.0$  eV for **4**, assuming the  $\lambda_i$  values are identical ( $\sim 0.7$  eV) for these dyads. A smaller excess energy in **4** is qualitatively compatible with the faster  $^1\text{CT}$  decay rates. However, it should be noted that the observed back-electron-transfer rates for these dyads are considerably fast in spite of the large excess energy in the Marcus inverted region. Although the presence of the inverted region has been experimentally demonstrated in many systems, the effect is known to be much less than that predicted on the basis of the classical Marcus theory,<sup>4</sup> indicating the importance of nuclear tunneling quantum effects<sup>24</sup> in the Marcus inverted region.

Transient triplet species,  $^3\text{LE}$  (naphthalimide) for **1** and **2**, and  $^3\text{CT}$  for **3**, were observed. The  $^3\text{CT}$  states were also observed for **4** with a lower contribution than those for **3**.

**Laser Photolysis of 2–4 in DMF.** The laser photolyses of **2–4** were also studied in a polar solvent, DMF. The generated  $^1\text{CT}$  was found to be short-lived in all cases. Although the lowest triplet state was predicted to be  $^3\text{CT}$  in this solvent (Table 2), neither  $^3\text{CT}$  nor  $^3\text{LE}$  could be observed.

The transient spectra for the picosecond-laser excitation of **3m** are shown in Figure 8 as a typical example. The spectrum is assigned to the  $^1\text{CT}$  state ( $\lambda_{\text{max}} = 414, 490$  nm for naphthalimide radical anion moiety and  $\lambda_{\text{max}} = 748$  nm for the donor radical cation moiety). The absorptions due to  $^1\text{CT}$  had almost disappeared ( $\tau = 20$  ps) within 500 ps after the laser excitation, indicating a very small fraction of  $^3\text{CT}$  state. In fact, no transient absorption was observed in the nanosecond-laser excitation. Similar results were obtained for **3p** ( $\tau = 11$  ps with  $\lambda_{\text{max}} = 413, 493, 749$  nm) and the other compounds ( $\tau = 100$  ps with  $\lambda_{\text{max}} = 411, 482, 670$  nm for **2m**,  $\tau = 46$  ps with  $\lambda_{\text{max}}$

$= 410, 483, 697$  nm for **2p**,  $\tau = 6.8$  ps with  $\lambda_{\text{max}} = 410, > 600$  nm for **4m**, and  $\tau = 6.5$  ps with  $\lambda_{\text{max}} = 411, > 600$  nm for **4p** in Figures S38–S40).

Thus, in DMF, both the generation and the decay of  $^1\text{CT}$  states are very fast and no triplet species was detected. The electron transfer for the charge-separation step from the excited singlet state is an exothermic process (1.2–1.7 eV) for all dyads. The back electron-transfer step in this solvent is much more exothermic ( $\Delta G_{\text{bet}} = -\Delta G_{\text{rip}}$ :  $\sim 2.2, 2.0, 1.5$  eV for **2, 3**, and **4**, Table 2). The observed lifetime of  $^1\text{CT}$  decreases in the sequence of **2** [ $\tau = 100$  ps (**2m**), 46 ps (**2p**)] → **3** [20 ps (**3m**), 11 ps (**3p**)] → **4** [6.8 ps (**4m**), 6.5 ps (**4p**)], which accords with the sequence of the decrease of  $\Delta G_{\text{rip}}$ , suggesting a small but important effect in the Marcus inverted region. The considerable increase in the CT decay rates in DMF compared to those in toluene would be ascribed to the increase of solvent contribution in the reorganization energy ( $\lambda_{\text{S}}$ : 0.4–0.5 eV for **1–3** in DMF, 0.03 eV in toluene in Table 3). Assuming that  $\lambda_i$  is identical ( $\sim 0.7$  eV) in both solvents, the reorganization energy  $\lambda_{\text{CT}}$  are estimated to be  $\sim 1.2$  eV in DMF for **1–4**. The excess energies ( $\Delta G_{\text{rip}} - \lambda_{\text{CT}}$ ) of the electron-transfer process ( $^1\text{CT} \rightarrow \text{GS}$ ) are considerably small in DMF in comparison with those in toluene; 0.3 eV (for **4**) to 1.0 eV (for **1**) in DMF, 1.0 eV (for **4**) to 1.8 eV (for **1**) in toluene, compatible with the faster decay rates in DMF in the Marcus inverted region.

**Topology Effect on the Lifetime of  $^1\text{CT}$  and  $^3\text{CT}$ .** The back-electron-transfer rates from both  $^1\text{CT}$  and  $^3\text{CT}$  to the ground states for the meta-isomers were found to be several times slower than those for the para-isomers. This was observed for all derivatives except **4** where the topology difference was minimized (Table 4). The redox potentials for both isomers are nearly same (Table 1). The averaged distance between the radical cation and the radical anion moieties are slightly longer in the para-isomers, which in turn renders the  $\Delta G_{\text{rip}}$  energy of the para-isomers higher than that of the meta-isomer in toluene (Table 2). The driving force of the back-electron transfer to the ground state ( $\Delta G_{\text{bet}} = -\Delta G_{\text{rip}}$ ) is therefore slightly more exothermic in the para-isomer in toluene. As discussed above, the back-electron-transfer process for the present system is in the Marcus inverted region. Therefore, the driving force term would predict the reverse order of what was observed. The observed decay rates can be rationalized by the pre-exponential term involving electronic interaction in the Marcus theory. The HOMO of the para-isomers has a large orbital coefficient on the Cp-carbon atom (see the formula of **3p** and **3p-HOMO** in Figure 2) in the donor moieties and a small coefficient even on the nitrogen (naphthalimide) atom, whereas they are absent in the meta-isomers. This would induce a small electronic interaction between the donor radical cation and the naphthalimide radical anion through a  $\sigma$ -type electronic interaction in the para-isomer, which would be visible on the carbon–nitrogen (naphthalimide) bond in HOMO of **3p**, or more clearly in HOMOs for para-isomers **1p–4p** in the SI. Such an electronic interaction must be much smaller in the meta-isomers.

**Distance Effect of Electron Transfer: 5m and 5p vs 3m and 3p.** Photolysis of **3m** and **3p** ( $R = \text{OMe}$ ) in toluene led to partial conversion to  $^3\text{CT}$ , which had lifetimes of several hundred nanoseconds. It is interesting to compare these results with those of the *p*-phenylene-extended analogues, **5m** and **5p**. The *p*-phenylene-bridge results in several changes affecting the radical ion pair energy ( $\Delta G_{\text{rip}}$ ). The redox potential term ( $E_{\text{ox}} - E_{\text{red}}$ ) in  $\text{CH}_2\text{Cl}_2$  contributes to stabilization of the radical ion pair by  $\sim 0.06$  eV mainly due to the decrease of  $E_{\text{ox}}$  (+0.21 V for **TPA(OMe)-Ph** in  $\text{CH}_2\text{Cl}_2$ ), whereas the distance ( $R$ , 11.7



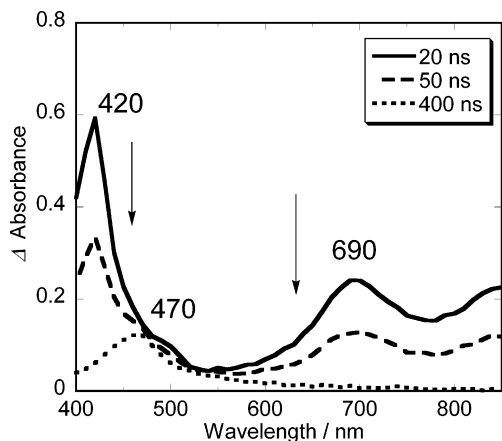


**Figure 9.** Transient spectra of **5m** after excitation of a nanosecond laser pulse (355 nm, fwhm: 4 ns) in toluene.

Å for **5m** and 12.9 Å for **5p** vs 7.5 Å for **3m** and 8.5 Å for **3p**) term largely destabilizes the ion-pair energy in **5** by 0.26 eV, an average of the meta- (0.29 eV) and the para-isomers (0.24 eV). As a consequence, the  $\Delta G_{\text{rip}}$  values of **5m** and **5p** become higher in energy by  $\sim 0.19$  eV than those of **3m** and **3p**. The same conclusion can be drawn from the  $E_{\text{CT}}$  values:  $E_{\text{CT}} = 2.23$  eV for **3**, 2.44 eV for **5** in comparison with  $E_{\text{T}}$  (naphthalimide) = 2.27 eV for both **3** and **5** (*vide supra*). Thus, the lowest triplet states in *p*-phenylene-bridged **5m** and **5p** are switched to the  $^3\text{LE}$  states (naphthalimide) in comparison with the  $^3\text{CT}$  state for **3m** and **3p**. Excitation of **5m** in toluene led to the  $^1\text{CT}$  state (420 nm for the naphthalimide radical anion and 690 nm for the radical cation, Figure 9, Figures S35–S37). The 690 nm band is somewhat shorter than **TPA(OMe)-Ph<sup>+</sup>** ( $\lambda_{\text{max}} = 756$  nm in Figure S26). The  $^1\text{CT}$  state has also an absorption in longer wavelength region ( $>800$  nm), which is partly due to the naphthalimide anion radical. These  $^1\text{CT}$  bands were almost completely replaced after 400 ns by the 470 nm band that can be clearly assigned to be  $^3\text{LE}$  (naphthalimide). The observation is in sharp contrast to that for **3**. In DMF, the lowest triplet state is predicted to be  $^3\text{CT}$  for both **3** and **5**. However, the  $^1\text{CT}$  exclusively decayed to the ground state as observed for other derivatives in DMF (*vide supra*).

**Acknowledgment.** We thank Iketani Science and Technology Foundation (No. 0191002-A) for financial support.

**Supporting Information Available:** Synthetic procedures and compounds data for **4** and **5**, figures of spectral data including absorption spectra of **1–5** in toluene (Figures S1–S5), fluorescence spectra of **1–3**, **5**, and model compounds (Figures S6–S15), phosphorescence spectra of **1–3**, **5**, and model compounds (Figures S16–S21), spectral change during the electrochemical reduction of **NI-Ph** and the oxidation of reference compounds (Figure S22–S26), transient absorption spectra for **1–5** in toluene and dioxane (Figures S27–S37), transient absorption spectra for **1–5** in DMF (Figures S38–S41), and a list of T-DFT calculation for **1–5** are available free of charge at <http://pubs.acs.org>.

## References and Notes

- (1) (a) Deisenhofer, J.; Michel, H. *Angew. Chem., Int. Ed. Engl.* **1989**, *28*, 829–847. (b) Huber, R. *Angew. Chem., Int. Ed. Engl.* **1989**, *28*, 848–869.
- (2) (a) Kavarnos, G. J. In *Fundamentals of Photoinduced Electron Transfer*; Wiley: New York, 1993. (b) Wasielewski, M. R. *J. Org. Chem.* **2006**, *71*, 5051–5066. (c) Gust, D.; Moore, T. A.; Moore, A. L.; Macpherson, A. N.; Lopez, A.; DeGraziano, J. M.; Gouni, I.; Bittersmann,

- E.; Seely, G. R.; Gao, F.; Nieman, R. A.; Ma, X. C.; Demanche, L. J.; Hung, S.-C.; Luttrull, D. K.; Lee, S.-J.; Kerrigan, P. K. *J. Am. Chem. Soc.* **1993**, *115*, 11141–11152. (d) van Dijk, S. L.; Wiering, P. G.; van Staveren, R.; van Ramesdonk, H. J.; Brouwer, A. M.; Verhoeven, J. W. *Chem. Phys. Lett.* **1993**, *214*, 502–506. (e) Osuka, A.; Yamada, H.; Ohno, T.; Nozaki, K. *Chem. Phys. Lett.* **1995**, *238*, 37–41. (f) Regev, A.; Galili, T.; Levernion, H.; Schuster, D. I. *J. Phys. Chem. A* **2006**, *110*, 8593–8598. (g) Palacios, R. E.; Kodis, G.; Herrero, C.; Ochoa, E. M.; Gervald, M.; Gould, S. L.; Kennis, J. T. M.; Gust, D.; Moore, T. A.; Moore, A. L. *J. Phys. Chem. B* **2006**, *110*, 25411–25420. (h) D'Souza, F.; Chitta, R.; Gadde, S.; Islam, D.-M. S.; Schumacher, A. L.; Zandler, M. E.; Araki, Y.; Ito, O. *J. Phys. Chem. B* **2006**, *110*, 25240–24250. (i) Cho, D. W.; Fujitsuka, M.; Sugimoto, A.; Yoon, U. C.; Mariano, P. S.; Majima, T. *J. Phys. Chem. B* **2006**, *110*, 11062–11068.

- (3) (a) Verhoeven, J. W.; van Ramesdonk, H. J.; Groeneveld, M. M.; Benniston, A. C.; Harriman, A. *Chem. Phys. Chem.* **2005**, *6*, 2251–2260. (b) Verhoeven, J. W. *J. Photochem. Photobiol. C* **2006**, *7*, 40–60.

- (4) (a) Anglos, D.; Bindra, V.; Kuki, A. *J. Chem. Soc., Chem. Commun.* **1994**, 213–215. (b) van Dijk, S. I.; Groen, C. P.; Hartl, F.; Brouwer, A. M.; Verhoeven, J. W. *J. Am. Chem. Soc.* **1996**, *118*, 8425–8432. (c) Widerrecht, G. P.; Svec, W. A.; Wasielewski, M. R.; Galili, T.; Levanon, H. *J. Am. Chem. Soc.* **2000**, *122*, 9715–9722. (d) Zeng, H.-P.; Wang, T.; Sandanayaka, A. S. D.; Araki, Y.; Ito, O. *J. Phys. Chem. A* **2005**, *109*, 4713–4720.

- (5) Harriman, A.; Mallon, L. J.; Ulrich, G.; Ziesel, R. *Chem. Phys. Chem.* **2007**, *8*, 1207–1214.

- (6) Ohno, T.; Nozaki, K.; Haga, M. *Inorg. Chem.* **1992**, *31*, 548–555.

- (7) Yoshimura, A.; Nozaki, K.; Ikeda, N.; Ohno, T. *J. Phys. Chem.* **1996**, *100*, 1630–1637.

- (8) (a) Yamamoto, T.; Nishiyama, M.; Koie, Y. *Tetrahedron Lett.* **1998**, *39*, 2367–2370. (b) Hamann, B. C.; Hartwig, J. F. *J. Am. Chem. Soc.* **1998**, *120*, 7369–7370. (c) Old, D. W.; Wolfe, J. P.; Buchwald, S. L. *J. Am. Chem. Soc.* **1998**, *120*, 9722–9723. (d) Hartwig, J. F.; Kuwatsura, M.; Hauck, S. I.; Shaughnessy, K. H.; Alcazar-Roman, L. M. *J. Org. Chem.* **1999**, *64*, 5575–5580.

- (9) Hoshino, Y.; Miyaura, N.; Suzuki, A. *Bull. Chem. Soc. Jpn.* **1988**, *61*, 3008–3010.

- (10) The percentage of excitation (355 nm) of naphthalimide chromophore for the para isomers: **1p**, 72%; **2p**, 62%; **3p**, 53%; **4p**, 33%; **5p**, 18%.

- (11) Demeter, A.; Bérces, T.; Biczók, L.; Wintgens, V.; Valat, P.; Kossanyi, J. *J. Phys. Chem.* **1996**, *100*, 2001–2011.

- (12) Wintgens, V.; Valat, P.; Kossanyi, J.; Demeter, A.; Biczók, L.; Bérces, T. *New J. Chem.* **1996**, *20*, 1149–1158.

- (13) (a) Korol'kova, N. V.; Val'kova, G. A.; Shigorin, D. N.; Shigalovskii, V. A.; Vostrova, V. N. *Russ. J. Phys. Chem.* **1990**, *64*, 206–209. (b) Wintgens, V.; Valat, P.; Kossanyi, J.; Biczók, L.; Demeter, A.; Bérces, T. *J. Chem. Soc. Faraday Trans.* **1994**, *90*, 411–421.

- (14) Wasielewski, M. R.; Johnson, D. G.; Svec, W. A.; Kersey, K. M.; Minsk, D. W. *J. Am. Chem. Soc.* **1988**, *110*, 7219–7221.

- (15) Spartan '06, Wavefunction, Inc., Irvine, CA.

- (16) Frisch, M. J.; Trucks, G. W.; Schlegel, H. B.; Scuseria, G. E.; Robb, M. A.; Cheeseman, J. R.; Montgomery, J. A., Jr.; Vreven, T.; Kudin, K. N.; Burant, J. C.; Millam, J. M.; Iyengar, S. S.; Tomasi, J.; Barone, V.; Mennucci, B.; Cossi, M.; Scalmani, G.; Rega, N.; Petersson, G. A.; Nakatsuji, H.; Hada, M.; Ehara, M.; Toyota, K.; Fukuda, R.; Hasegawa, J.; Ishida, M.; Nakajima, T.; Honda, Y.; Kitao, O.; Nakai, H.; Klene, M.; Li, X.; Knox, J. E.; Hratchian, H. P.; Cross, J. B.; Bakken, V.; Adamo, C.; Jaramillo, J.; Gomperts, R.; Stratmann, R. E.; Yazyev, O.; Austin, A. J.; Cammi, R.; Pomelli, C.; Ochterski, J. W.; Ayala, P. Y.; Morokuma, K.; Voth, G. A.; Salvador, P.; Dannenberg, J. J.; Zakrzewski, V. G.; Dapprich, S.; Daniels, A. D.; Strain, M. C.; Farkas, O.; Malick, D. K.; Rabuck, A. D.; Raghavachari, K.; Foresman, J. B.; Ortiz, J. V.; Cui, Q.; Baboul, A. G.; Clifford, S.; Cioslowski, J.; Stefanov, B. B.; Liu, G.; Liashenko, A.; Piskorz, P.; Komaromi, I.; Martin, R. L.; Fox, D. J.; Keith, T.; Al-Laham, M. A.; Peng, C. Y.; Nanayakkara, A.; Challacombe, M.; Gill, P. M. W.; Johnson, B.; Chen, W.; Wong, M. W.; Gonzalez, C.; and Pople, J. A. *Gaussian 03*, revision C.02; Gaussian, Inc.: Wallingford, CT, 2004.

- (17) (a) Weller, A. *Z. Phys. Chem. Neu. Folg.* **1982**, *133*, 93–98. (b) Lor, M.; Viaene, L.; Pilot, R.; Fron, E.; Jordens, S.; Schweitzer, G.; Weil, T.; Müllen, K.; Verhoeven, J. W.; Van der Auweraer, M.; De Schryver, F. C. *J. Phys. Chem. B* **2004**, *108*, 10721–10731. (c) Williams, R. M.; Koeberg, M.; Lawson, J. M.; An, Y.-Z.; Rubin, Y.; Paddon-Row, M. N.; Verhoeven, J. W. *J. Org. Chem.* **1996**, *61*, 5055–5062.

- (18) Oevering, H.; Paddon-Row, M. N.; Heppener, M.; Oliver, A. M.; Cotsaris, E.; Verhoeven, J. W.; Hush, N. S. *J. Am. Chem. Soc.* **1987**, *109*, 3258–3269.

- (19) Marcus, R. A.; Sutin, N. *Biochim. Biophys. Acta* **1985**, *811*, 265–322.

- (20) Demeter, A.; Biczók, L.; Bérces, T.; Wintgens, V.; Valat, P.; Kossanyi, J. *J. Phys. Chem.* **1993**, *97*, 3217–3224.

- (21) (a) Okada, T.; Karaki, I.; Matsuzawa, E.; Mataga, N.; Sakata, Y.; Misumi, S. *J. Phys. Chem.* **1981**, *85*, 3957–3960. (b) van Willigen, H.;

Jones, H. G.; Farahat, M. S. *J. Phys. Chem.* **1996**, *100*, 3312–3316. (c) Gould, I. R.; Boiani, J. A.; Gaillard, E. B.; Goodman, J. L.; Farid, S. *J. Phys. Chem. A* **2003**, *107*, 3515–3524.

(22) After 30 ps from laser excitation of **NI-Ph** in toluene, the observable species is only the triplet state of **NI-Ph**, showing the rapid intersystem crossing of the **NI-Ph** chromophore (less than a few ps).

(23) (a) Hasharoni, K.; Levanon, H.; Greenfield, S. R.; Gosztola, D. J.; Svec, W. A.; Wasielewski, M. R. *J. Am. Chem. Soc.* **1995**, *117*, 8055–8056. (b) Dance, Z. E. X.; Mi, Q.; McCamant, D. W.; Ahrens, M. J.; Ratner, M. A.; Wasielewski, M. R. *J. Phys. Chem. B* **2006**, *110*, 25163–25173.

(24) (a) Jortner, J. *J. Chem. Phys.* **1976**, *64*, 4860–4867. (b) Bixon, M.; Jortner, J. *Adv. Chem. Phys.* **1999**, *106*, 35–202.